The effects of welding-induced residual stress on the buckling collapse behaviours of stiffened panels

Shen Li & Simon Benson
Marine, Offshore and Subsea Technology Group, School of Engineering, Newcastle University, UK

ABSTRACT: An assessment is conducted in this paper for the effects of welding-induced residual stress on the elastoplastic buckling collapse behaviour of stiffened panels subjected to in-plane compression. A series of nonlinear finite element analyses (NLFEA) are completed which covers a range of plate slenderness ratios ($\beta = 1.0\sim4.0$) and column slenderness ratios ($\lambda = 0.2\sim1.2$) typical in marine application. The finite element models incorporate an idealised distribution of welding-induced residual stress with average severity. The numerical investigation indicates a reduced ultimate strength and increased ultimate strain due to the residual stress, as compared with the initial stress-free condition. Hence, a set of design formulae are proposed with the aid of regression analysis to predict the ultimate strength reduction and ultimate strain variation. The proposed design formulae are employed in combination with an empirical load-shortening curve formulation and simplified progressive collapse method to predict the ultimate bending capacity reduction of a box girder model. Validation is completed through equivalent finite element analysis.

1 INTRODUCTION

The assessment of ultimate ship hull strength is usually completed using the simplified progressive collapse method, as codified in the Common Structural Rule (CSR) issued by IACS (2019). One of the key steps in the progressive collapse analysis is the estimation the structural components' elastoplastic buckling behaviour under in-plane compression, which is normally represented by a load-shortening curve. A wide range of methodology can be employed to predict the compressive load-shortening curves of stiffened panels, including analytical approach (Dow and Smith, 1986; Yao and Nikolov, 1991 & 1992; Ueda and Rashed, 1984; Ueda et al., 1984), numerical simulation (Benson et al, 2013; Li et al., 2019) and empirical formulation (Li et al., 2020).

Among various methodology, the empirical formulation introduced by Li et al. (2020) is highly efficient, as only the basic dimensionless parameters are involved, in comparison to the analytical approach with rather complicated derivation and computationally expensive numerical simulation.

Following the previous development in Li et al. (2020), this paper aims to enhance the empirical formulation to accommodate the effects of welding-induced residual stress. A series of nonlinear finite element analyses (NLFEA) covering seven plate slenderness ratios ($\beta = 1.0\sim4.0$) and six column slenderness ratios ($\lambda = 0.2\sim1.2$) are completed to explore the influence of residual stress on load-shortening behaviours of stiffened panels. Based on the NLFEA results, a set of design equations are proposed to evaluate the ultimate strength reduction and ultimate strain variation due to welding-induced residual stress. The proposed design equations are employed in conjunction with empirical load-shortening curve formulation and simplified progressive collapse method to predict the ultimate bending capacity reduction of a box girder model. Validation is completed through equivalent finite element analysis.

2 BACKGROUND

During the welding process, the welding metal is melted with the mother plates until solidification (Yao and Fujikubo, 2016). Skrinkage of the stiffened panels would occur at the solidified part which is constrained by the surrounding unmelted part. As a result, the tensile stress is induced in the solidified part and the compressive stress is developed at the neighbouring part so as to achieve an equilibrium condition. In short, the residual stress caused by welding is induced as tension near the welding line, whereas a compressive stress field is developed in the adjacent part.

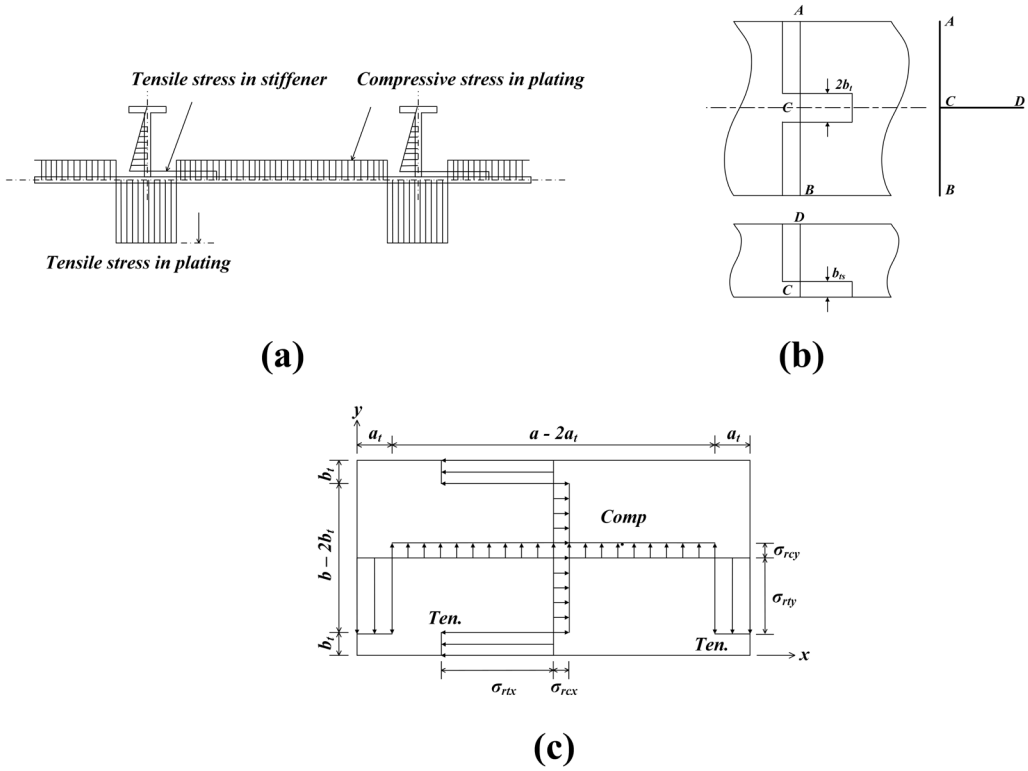

Figure 1. Idealised distribution of the welding-induced residual stress in stiffened panels

Smith et al. (1991) suggested a simplified welding-induced residual stress distribution for stiffened panels (Figure 1a), in which the residual stress field was idealised as tension and compression blocks. In addition, a triangular distribution shape was assumed for the compressive stress field of stiffener's web, while the tensile stress field was taken as a rectangular strip near the intersection with plating. Similar distribution was given by Yao and Fujikubo (2016) for fillet welding (Figure 1b). However, an uniform distribution was assumed for the compressive stress field along the height of the stiffener's web. A more elaborated distribution pattern for the plating was given by Paik and Thayamballi (2003) considering the residual stress in both longitudianl and transverse directions (Figure 1c).

Since the residual stress is self-equilibrating, the equilibrium condition gives the relationship of Equation (1). To determine the magnitude of the residual stress, Yao (1980) suggested that the width of tensile block can be expressed as a function of plating thickness, web thickness and the weld heat input. Meanwhile, the tensile yield stress is equal to the material yield stress in the case of ordinary steel (Yao et al., 1998). An empirical formula was given by Smith et al. (1991) to estimate the compressive residual stress (Equation 2 to 4). Three different severities (slight, average and severe) were suggested.

$$2b_t\sigma_{rtx} = (b - 2b_t)\sigma_{rcx} \quad (1)$$

$$\sigma_{rcx} = 0.05\sigma_{Yp}\ (slight) \quad (2)$$

$$\sigma_{rcx} = 0.15\sigma_{Yp}\ (average) \quad (3)$$

$$\sigma_{rcx} = 0.30\sigma_{Yp}\ (severe) \quad (4)$$

Several case studies may be found in the litarature on the effects of welding-induced residual stress. Gannon et al. (2016) conducted a nonlinear collapse analysis on tee-bar and angle-bar stiffened plates under compression considering the welding-induced residual stress. A three-dimensional thermo-elasto-plastic finite element analysis was carried out to simulate the residual stress due to welding. The resutls suggested that the ultimate strength may be reduced by 12.5% because of the residual stress. Hansen (1996) concluded that residual stress may lead to decrease of ultimate strength by 25%, while Gordo and Guedes Soares (1993) found that the ultimate strength was reduced by 10% when the compressive residual stress in the plate was taken as 20% of the yield stress. Regarding to the hull girder strength, Gannon et al. (2012) reported that the hull girder strength can be reduced by 3.3% in the case that the ultimate strength of its component stiffened panels was decreased by 11%. As suggested by the literature survey, it is generally accepted that the welding-induced residual stress would lead to the reduction of ultimate compressive strength of stiffened panels. However, a practical solution to consider the welding-induced residual stress in the ultimate limit state design of stiffend plating structures is lacking.

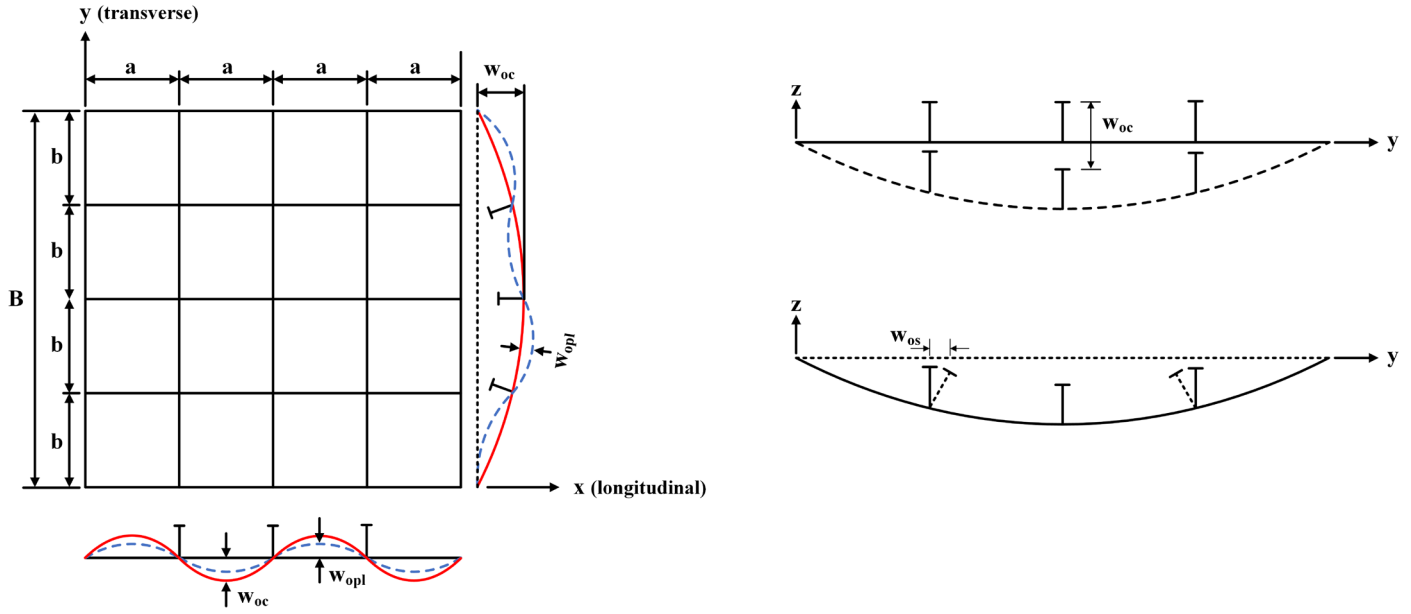

Figure 2. Schematic view of the initial distortions

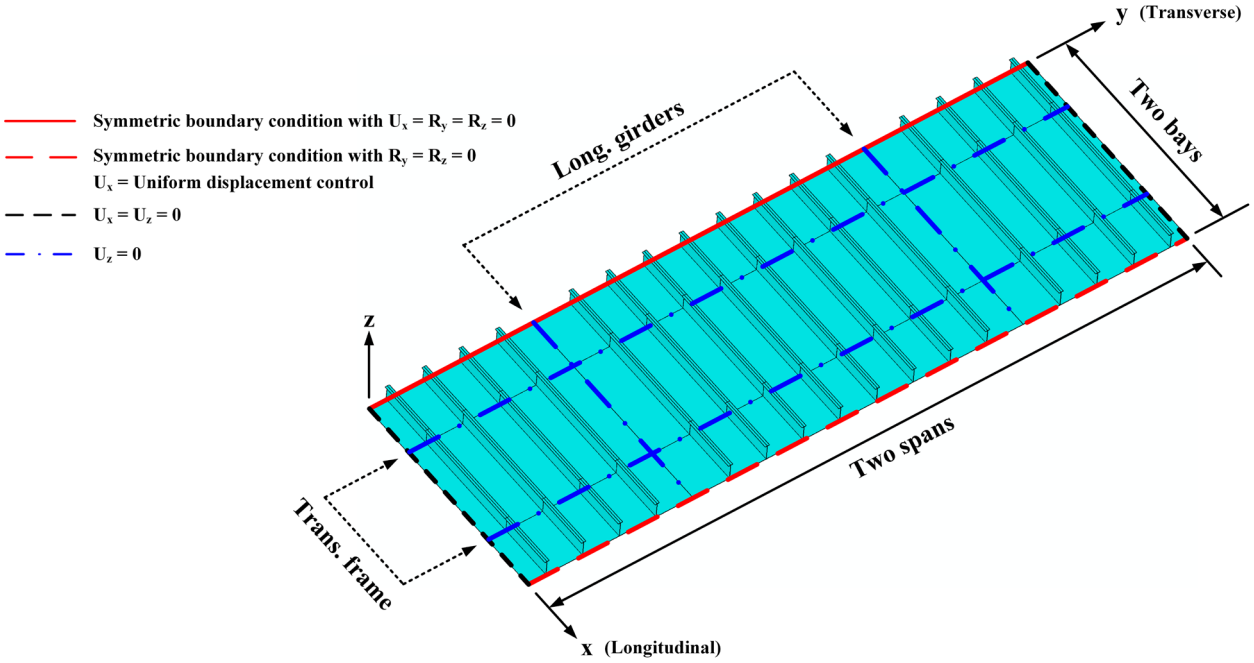

Figure 3. Boundary conditions of FE stiffened panel models

3 NONLINEAR FINITE ELEMENT ANALYSIS

3.1 *Scope of analysis*

Nonlinear finite element analysis is carried out for a series of stiffened panels with and without residual stress under compressive load, in which the following parameters are varied systematically giving a total of 42 stiffened panels and 84 test cases:

- Plate slenderness ratio $\beta = b/t\sqrt{\sigma_{Yeq}/E}$ = 1.0, 1.5, 2.0, 2.5, 3.0, 3.5, 4.0;
- Column slenderness ratio $\lambda = a/\pi r\sqrt{\sigma_{Yeq}/E}$ = 0.2, 0.4, 0.6, 0.8, 1.0, 1.2;
- Stiffener area ratio $A_s/A = A_s/(A_s+bt) = 0.2$ where As is the stiffener cross-sectional area;
- Stiffener shape: all calculations refer to tee-bar stringers, which corresponds to the 114mm × 44.5mm Admiralty long-stalk tee bar section;
- Material property: the yield strength and Young's modulus in all calculations are 324MPa and 207000MPa respectively. An elastic-perfectly plastic behaviour is assumed;
- Initial distortion: local plate distortion w_{opl}, column-type distortion w_{oc} and stiffener sideway distortion w_{os} as defined by Equation (5) to (7) and schematically shown in Figure 2;
- Residual stress: it is only considered for the plating in the longitudinal direction following Figure 1(c). The width of tensile stress block b_t is taken assuming that the tensile residual stress equals the material yields stress and compressive residual stress corresponds an average-level magnitude as given by Equation (3) (More details in Appendix).

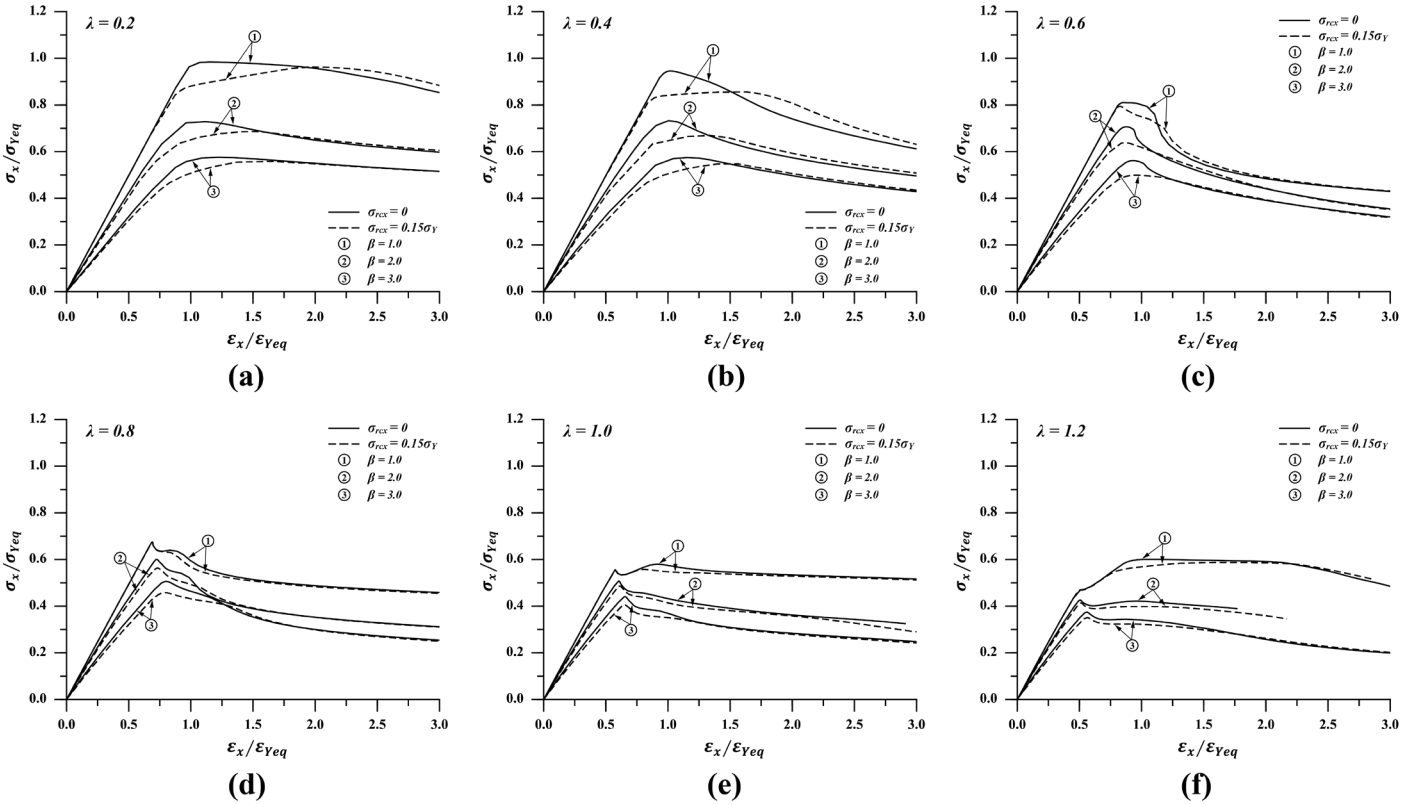

Figure 4. Selected load-shortening curves of stiffened panels with and without welding residual stress

$$w_{opl} = A_o sin\left(\frac{m\pi x}{a}\right) sin\left(\frac{\pi y}{b}\right) \quad (5)$$

$$m = \frac{a}{b} + 1$$

$$w_{oc} = B_o sin\left(\frac{\pi x}{a}\right) sin\left(\frac{\pi y}{B}\right) \quad (6)$$

$$w_{os} = C_o \frac{z}{h_w}\left[0.8sin\left(\frac{\pi x}{a}\right) + 0.2sin\left(\frac{i\pi x}{a}\right)\right] \quad (7)$$

$$i = a/h_w + 1$$

$$A_o = 0.1\beta^2 t$$

$$B_o = 0.0015a$$

$$C_o = 0.0015a$$

3.2 *Finite element modelling*

It was discussed by ISSC (2012) that the constrain of the end-rotation of stiffeners may over-estimate the ultimate compressive strength of stiffened panels. Meanwhile, Smith et al. (1991) indicated that the interaction between longitudinal adjacent structures should be considered. Thus, a two bays/two span model with eight identical stiffeners in each span is employed (Figure 3). The longitudinal girder and transverse frame are modelled with boundary condition constraining the out-of-plane movement. The present model extent allows for the end-rotation of stiffeners and the interactions between the adjacent structures in the longitudinal direction and may be a reasonable representation of typical continuous ship grillages.

The FE model is discretised with four-node shell element (S4R in ABAQUS) with reduced integration. For the local plating, the element number in the longitudinal direction is taken as 50λ dependent on the column slenderness ratio, while ten elements are employed in the transverse direction for all cases giving a characteristic plating mesh size of 50mm × 50mm. For the stiffener, six elements are used in both stiffener's web and flange.

The welding-induced residual stress are modelled by applying an initial stress field. An average-level magnitude is considered. A relaxation step is applied for the self-equilibrium of the initial stress field.

3.3 *Results and discussions*

A selection of the load-shortening curves of the tested stiffened panels are shown in Figure 4 to compare the predictions with and without welding residual stress. From these comparisons, the following observations can be made:

- A reduced initial stiffness is observed for all tested cases as a result of the welding residual stress. However, the stiffness reduction is relatively insignificant, which may therefore be discarded in the ultimate limit state assessment;
- The ultimate compressive strength of stiffened panels is degraded due to the residual stress. A contour plot illustrating the strength reduction of different stiffened panel configurations is given in Figure 5 by a cubic interpolation of the obtained numerical results. Comparison with the CSR method is given where the effect of residual stress

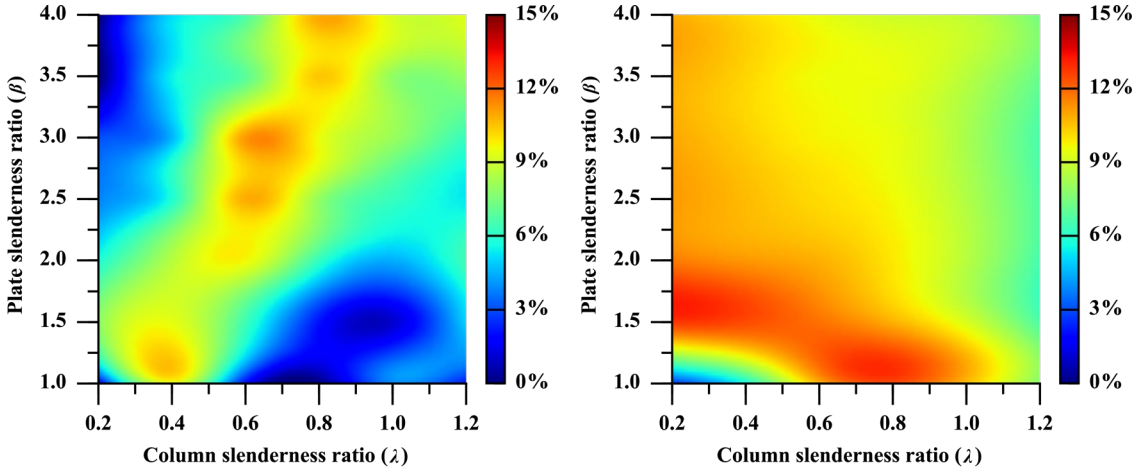

(a) NLFEA (b) CSR

Figure 5. Ultimate strength reduction caused by welding residual stress (Cubic interpolation)

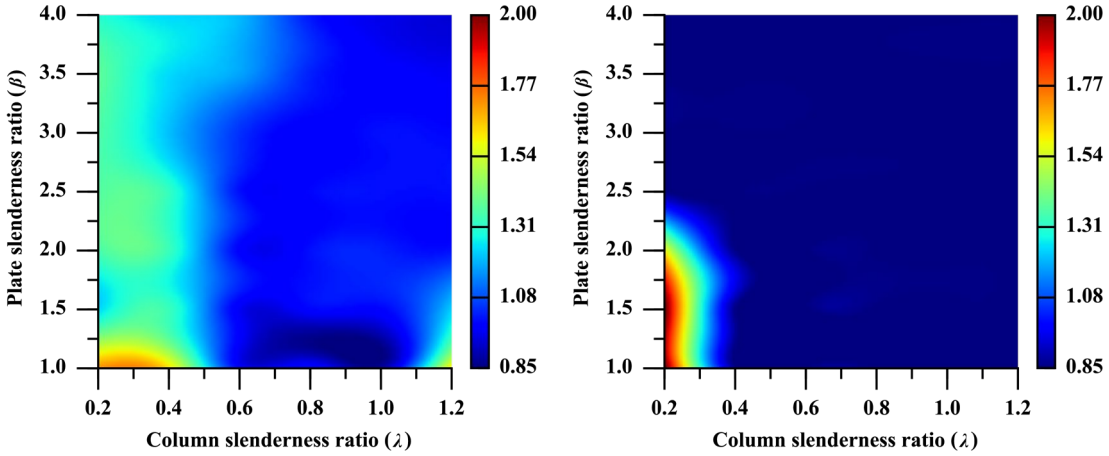

(a) NLFEA (b) CSR

Figure 6. Ultimate strain variation caused by welding residual stress (Cubic interpolation)

is accounted by modifying the edge function, as proposed by Gordo and Guedes Soares (1993). A maximum reduction of 11.2% is induced in the numerical simulation. The reduction is less considerable for stiffened panels with a combination of low λ and high β or combination of high λ and low β. However, the corresponding CSR prediction is generally overestimated;

- It appears that the collapse of stiffened panels generally takes place at a higher strain due to the welding residual stress, which is more substantial for low plate and column slenderness panels ($\beta \leq 1.5$ & $\lambda \leq 0.4$) as shown in Figure 6. This may be due to the presence of initial tensile stress field which induces certain hardening effect (Khan and Zhang, 2011).
- The post-collapse behaviour is unaffected by the residual stress with nearly identical response path.

4 DESIGN EQUATIONS

Design equations are proposed in the general form given by Equation (8) for predicting the ultimate strength reduction. Least-square regression is performed for different column slenderness ratios and thus six sets of coefficients are derived based on the present dataset, as summarised in Table 1 where the goodness-of-fit (R^2) is also indicated. For the prediciton of stiffened panels with a column slenderness ratio other than those tested in the present study, an interpolation between the results may be used:

In regard to ultimate strain variation, the same four-order polynomial form is adopted (Equation 9). However, regression analysis is only conducted for column slenderness ratio $\lambda = 0.2$ and 0.4, since only an insignificant ultimate strain variation is induced by the residual stress as indicated in Figure 7. Hence, two sets of coefficients are suggested and summarised in Table 2.

The statistical correlation of the prediction between the proposed design equations and the present NLFEA is shown in Figure 7. A good agreement is obtained with a mean value of 0.9804 and COV of 0.0930 respectively for strength reduction prediction and a mean value of 1.0021 and COV of 0.0282 for collapse strain variation prediction.

$$\frac{\sigma_{xu}-\sigma_{xu}^{R}}{\sigma_{xu}} = \sum_{i=0}^{4} C_i \beta^i \quad (8)$$

$$\frac{\varepsilon_{xu}^{R}}{\varepsilon_{xu}} = \sum_{i=0}^{4} D_i \beta^i \quad (9)$$

5 APPLICATION

The proposed design equations are applied in combination with the empirical load-shortening curve (LSC) formulation introduced by Li et al. (2020) and simplified progressive collapse method (ProColl) to predict the ulimate bending strength of a welded box girder model. Validation is performed through a comparison with equavilent NLFEA. The case study model was tested originally by Gordo and Guedes Soares (2013). The dimensions of the box girder model is illustrated in Figure 8. The model is made of mild steel with yield stress of 270 MPa and Young's modulus of 200000 MPa.

Detailed derivation of the empirical formulation can refer to Li et al. (2020). To accommodate the influence of welding residual stress on overall load-shortening behaviour, the formulation is modified for low slenderness stiffened panels ($\lambda \leq 0.4$) as schematically illustrated in Figure 9 and given by Equation (10) to (12). On the other hand, the LSC of high slenderness stiffened panels ($\lambda > 0.4$) follows the original formulation. The compressive ultimate strength of structural members are estimated by Zhang and Khan formula (2009).

The initial stress field of the FE model after relaxation is shown in Figure 10. Figure 11 compares the collapse mode of the box girder model with and without residual stress. In both cases, the collapse of the box girder is primarily induced by beam-column buckling. A comparison of the bending moment/curvature curves is given in Figure 12. Although the pre-collapse bending stiffness is underestimated by the NLFEA, which may be attributed to multi-frame configuration of the box girder model, there is close correlation on the reduction of ultimate bending capacity of the case study model as given in Table 3. The accuracy of the proposed design equations may therefore be verified.

Table 1. Coefficients of the proposed design equations to evaluate the ultimate strength reduction

	C_0	C_1	C_2	C_3	C_4	R^2
$\lambda = 0.2$	-0.454	0.868	-0.497	0.1161	-0.00973	0.9404
$\lambda = 0.4$	-0.115	0.432	-0.292	0.0762	-0.00687	0.9655
$\lambda = 0.6$	0.117	-0.333	0.337	-0.1107	0.01163	0.9701
$\lambda = 0.8$	0.059	-0.190	0.178	-0.0518	0.00499	0.9944
$\lambda = 1.0$	0.534	-0.993	0.654	-0.1727	0.01612	0.9842
$\lambda = 1.2$	-0.256	0.511	-0.301	0.0752	-0.00661	0.9747

Table 2. Coefficients of the proposed design equations to evaluate the ultimate strain variation

	D_0	D_1	D_2	D_3	D_4	R^2
$\lambda = 0.2$	5.740	-7.49	4.47	-1.117	0.0996	0.9104
$\lambda = 0.4$	3.777	-4.05	2.45	-0.644	0.0612	0.9573

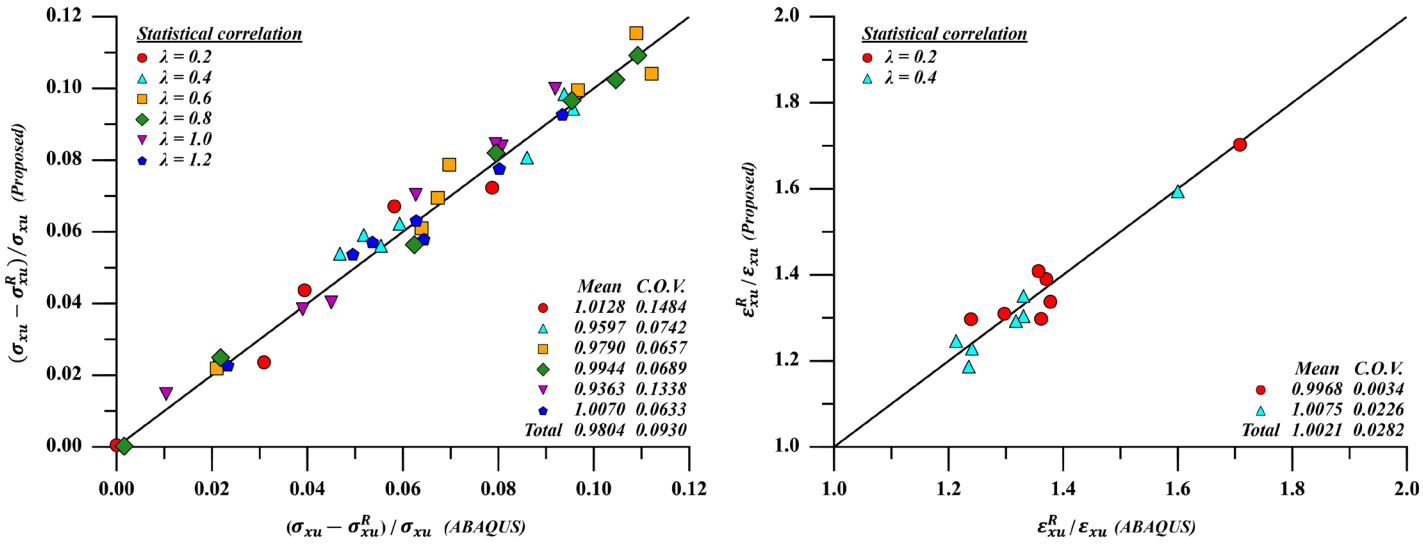

(a) **(b)**

Figure 7. Correlation of the prediction by proposed design equations and NLFEA

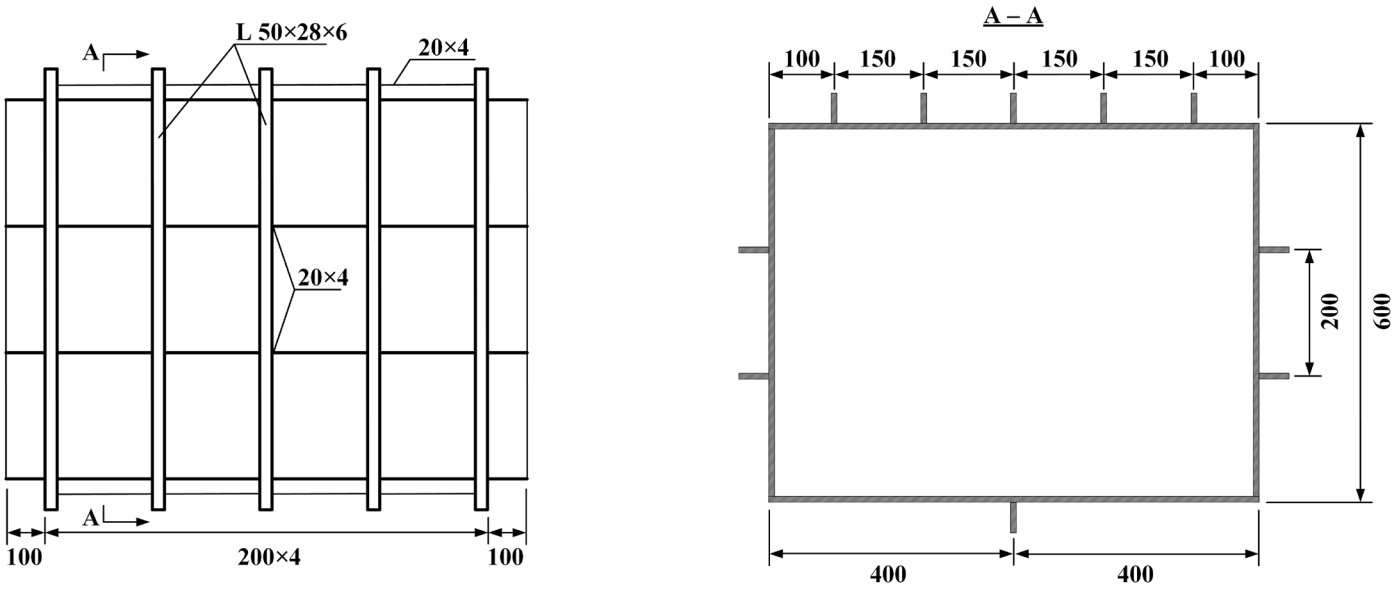

Figure 8. Schematic illustration of the case study model

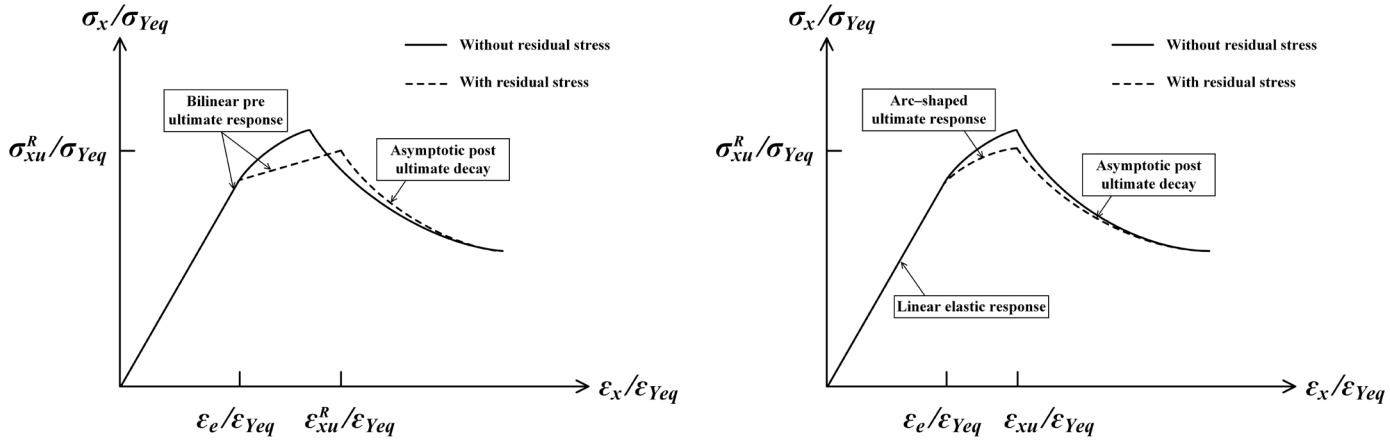

(a) $\lambda \leq 0.4$ **(b) $\lambda > 0.4$**

Figure 9. Empirical load-shortening curve formulation

$$\frac{\sigma_x}{\sigma_{Yeq}} = \bar{E}_{To}\frac{\varepsilon_x}{\varepsilon_{Yeq}} \tag{10}$$

$$\frac{\sigma_x}{\sigma_{Yeq}} = \bar{E}_T\left(\frac{\varepsilon_x}{\varepsilon_{Yeq}} - \frac{\varepsilon_e}{\varepsilon_{Yeq}}\right) + \frac{\sigma_e}{\sigma_{Yeq}} \tag{11}$$

$$\frac{\sigma_x}{\sigma_{Yeq}} = C\frac{\sigma_{xu}^R}{\sigma_{Yeq}} + (1-C)\frac{\sigma_{xu}^R}{\sigma_{Yeq}}exp\left(\frac{\varepsilon_{xu}^R}{\varepsilon_{Yeq}} - \frac{\varepsilon_x}{\varepsilon_{Yeq}}\right) \tag{12}$$

where

$$\frac{\varepsilon_{xe}}{\varepsilon_{Yeq}} = \frac{\varepsilon_{xu}}{\varepsilon_{Yeq}} + Rsin[-tan^{-1}(\bar{E}_{To})]$$

$$R = \frac{cos[tan^{-1}(\bar{E}_{To})]\left(\bar{E}_T\frac{\varepsilon_{xu}}{\varepsilon_{Yeq}} - \frac{\sigma_{xu}}{\sigma_{Yeq}}\right)}{1 - cos[tan^{-1}(\bar{E}_{To})]}$$

$$C = \left(0.7834 - 0.3174\sqrt{\lambda} - \frac{0.0060}{\beta^2}\right)\Big/\left(1 - \frac{\sigma_{xu} - \sigma_{xu}^R}{\sigma_{xu}}\right)$$

$$\frac{\varepsilon_{xu}}{\varepsilon_{Yeq}} = -0.0004 + 1.005\lambda - 1.3126\lambda^2 + 1.7101/\sqrt{\beta}$$

$$\frac{\varepsilon_{xu}}{\varepsilon_{Yeq}} = -0.3752\,\lambda/\sqrt{\beta} - 0.7337/\beta$$

$$\frac{\varepsilon_{xu}}{\varepsilon_{Yeq}} = \frac{\varepsilon_{xu}}{\varepsilon_{Yeq}} \times \frac{\varepsilon_{xu}^R}{\varepsilon_{xu}}$$

$$\frac{\sigma_{xu}^R}{\sigma_{Yeq}} = \frac{\sigma_{xu}}{\varepsilon_{Yeq}} \times \left(1 - \frac{\sigma_{xu} - \sigma_{xu}^R}{\sigma_{xu}}\right)$$

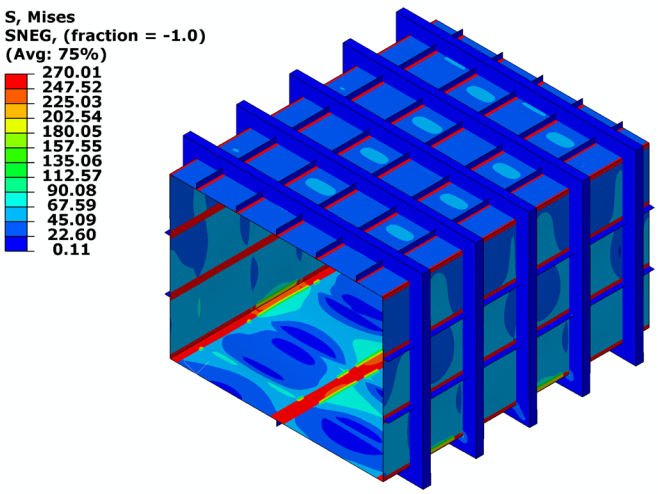

Figure 10. Initial stress field of box girder model

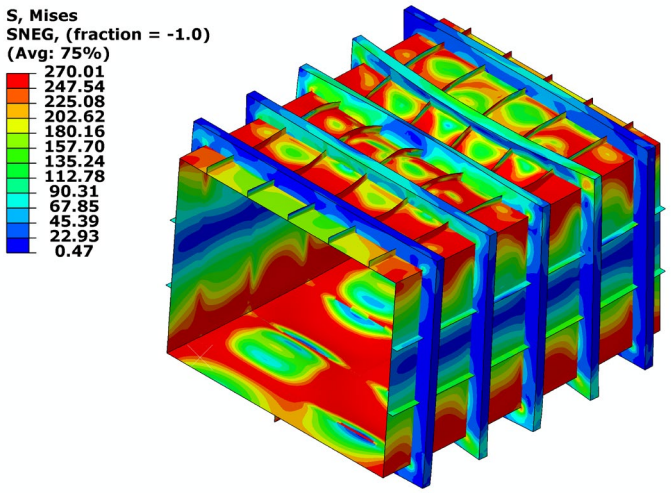

(a) Ultimate limit state of box girder with initial stress

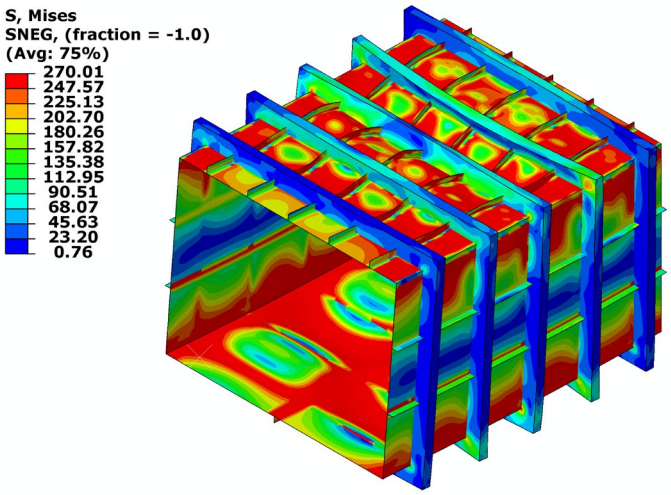

(b) Ultimate limit state of box girder with initial stress

Figure 11. Contour plots of box girder FE model

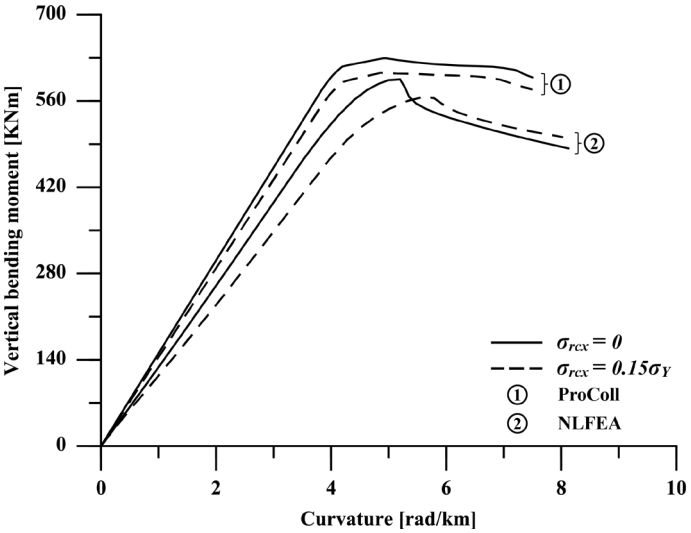

Figure 12. Comparison of bending moment/curvature curves

Table 3. Summary of the computed ultimate bending strength

	ProColl (KNm)	NLFEA (KNm)
Without residual stress	629.5752	595.1840
With residual stress	605.5636	566.9330
Reduction	-3.81%	-4.75%

6 CONCLUSIONS

A systematic nonlinear finite element analysis covering a range of plate slenderness ratio ($\beta = 1.0\sim4.0$) and column slenderness ratios ($\lambda = 0.2\sim1.2$) is conducted to assess the effect of welding residual stress. The finite element models incorporate an idealised distribution of welding-induced residual stress with average severity. Design formulae are proposed for prediction the collapse strength reduction and ultimate strain variation caused by residual stress. Application is presented to evaluate the ultimate bending strength of a welded box girder model. From this study, the following conclusion may be drawn:

- The welding-induced residual stress would deteriorate the ultimate compressive strength of stiffened panels and furthermore leads to a considerable variation of the ultimate strain for stock panels.
- The proposed design equations provide an efficient and accurate way to assess the effects of welding-induced residual stress on the progressive collapse behavior of stiffened panels;
- The design equations can be incorporated with the empirical formulation (Li et al., 2019b) to predict load-shortening curves of stiffened panels considering welding stress. The application in box girder ultimate bending strength prediction has demonstrated the accuracy of the proposed equations.

REFERENCES

18th ISSC, 2012. Ultimate Strength, Rostock, Germany.

Benson S, Downes J, Dow RS. 2013. Load shortening characteristics of marine grade aluminium alloy plates in longitudinal compression. *Thin-Walled Structures*, 70, 19–32.

Dow RS, Smith CS. 1986. FABSTRAN: A computer program for frame and beam static and transient response analysis (Nonlinear). ARE report TR86205.

Gannon L, Liu Y, Pegg N, Smith MJ, 2012. Effect of welding-induced residual stress and distortion on ship hull girder ultimate strength. *Marine Structures*, 28, 25–49.

Gannon L, Liu Y, Pegg N, Smith MJ, 2016. Nonlinear collapse analysis of stiffened plates considering welding-induced residual stress and distortion. *Ships and Offshore Structures*, 11, 228–244.

Gordo JM, Guedes Soares C, 1993. Approximate load shortening curves for stiffened plates under uniaxial compression. *In Proceeding: Integrity of Offshore Structures (Faulkner et al, Eds.)*, UK

Gordo JM, Guedes Soares C, 2013. Experiments on three mild steel box girders of different spans under pure bending moment. *In Proceeding: 4th International Conference on Marine Structures*, Helsinki, Finland.

Hansen AM, 1996. Strength of midship sections. *Marine Structures*, 9, 471–494.

International Association of Classification Societies (IACS). 2019. *Common Structural Rules for Bulk Carriers and Oil Tankers*.

Khan I, Zhang SM, 2011. Effects of welding-induced residual stress on ultimate strength of plates and stiffened panels. *Ships and Offshore Structures*, 6, 297–309.

Li S, Hu ZQ, Benson S. 2019. An analytical method to predict the buckling and collapse behaviour of plates and stiffened panels under cyclic loading. *Engineering Structures*, 199, 109627.

Li S, Kim DK, Benson S. 2020. An adaptable algorithm to predict the load-shortening curves of stiffened panels in compression. *In Proceeding: 5th International Conference on Ships and Offshore Structures*, Glasgow, UK.

Paik JK, Thayamballi, AK, 2003. Ultimate limit state design of steel-plated structures, John Wiley & Sons, Chichester, UK.

Smith CS, Anderson N, Chapman JC, Davidson PJ, Dowling PJ. 1991. Strength of stiffened plating under combined compression and lateral pressure. *Transactions of Royal Institution of Naval Architects*, 131–147.

Ueda Y, Rashed SMH. 1984. The idealized structural unit method and its application to deep girder structures. *Computers & Structures*, 18, 277 – 293.

Ueda Y, Rashed S, Paik JK. 1984. Plate and stiffened panel units of the idealized structural unit method under in-plane loading. *Journal of the Society of Naval Architects of Japan*, 156, 366–376.

Yao T, Fujikubo M, 2016. Buckling and ultimate strength of ship and ship-like floating structures, Elsevier.

Yao T, 1980. Compressive ultimate strength of structural members in ship structure. PhD thesis, Osaka University, Japan (in Japanese).

Yao T, Fujikubo M, Yanagihara D, Varghese B, Niho O, 1998. Influences of welding imperfections on buckling/ultimate strength of ship bottom plating subjected to combined bi-axial thrust and lateral pressure. *In Proceeding: International symposium on thin-walled structures*, Singapore.

Yao T, Nikolov P. 1991. Progressive collapse analysis of a ship's hull under longitudinal bending (1st report). *Journal of the Society of Naval Architects of Japan,* 170, 449 – 461.

Yao T, Nikolov P. 1992. Progressive collapse analysis of a ship's hull under longitudinal bending (2nd report. *Journal of the Society of Naval Architects of Japan,* 172, 437 – 446.

Zhang S, Khan I. 2009. Buckling and ultimate capability of plates and stiffened panels in axial compression. *Marine Structures*, 22, 791–808.

APPENDIX

No.	a [mm]	b_p [mm]	t_p [mm]	h_w [mm]	t_w [mm]	b_f [mm]	t_f [mm]	σ_{Yeq} [MPa]	β	λ	A_s/A	b_t [mm]
1	593.7	311.1	12.3	104.8	5.1	44.5	9.5	324.0	1.0	0.2	0.2	20.3
2	1187.4	311.1	12.3	104.8	5.1	44.5	9.5	324.0	1.0	0.4	0.2	20.3
3	1781.1	311.1	12.3	104.8	5.1	44.5	9.5	324.0	1.0	0.6	0.2	20.3
4	2374.8	311.1	12.3	104.8	5.1	44.5	9.5	324.0	1.0	0.8	0.2	20.3
5	2968.5	311.1	12.3	104.8	5.1	44.5	9.5	324.0	1.0	1.0	0.2	20.3
6	3562.2	311.1	12.3	104.8	5.1	44.5	9.5	324.0	1.0	1.2	0.2	20.3
7	586.5	381.0	10.0	104.8	5.1	44.5	9.5	324.0	1.5	0.2	0.2	24.8
8	1173.1	381.0	10.0	104.8	5.1	44.5	9.5	324.0	1.5	0.4	0.2	24.8
9	1759.6	381.0	10.0	104.8	5.1	44.5	9.5	324.0	1.5	0.6	0.2	24.8
10	2346.2	381.0	10.0	104.8	5.1	44.5	9.5	324.0	1.5	0.8	0.2	24.8
11	2932.7	381.0	10.0	104.8	5.1	44.5	9.5	324.0	1.5	1.0	0.2	24.8
12	3519.3	381.0	10.0	104.8	5.1	44.5	9.5	324.0	1.5	1.2	0.2	24.8
13	582.4	440.0	8.7	104.8	5.1	44.5	9.5	324.0	2.0	0.2	0.2	28.7
14	1164.7	440.0	8.7	104.8	5.1	44.5	9.5	324.0	2.0	0.4	0.2	28.7
15	1747.1	440.0	8.7	104.8	5.1	44.5	9.5	324.0	2.0	0.6	0.2	28.7
16	2329.4	440.0	8.7	104.8	5.1	44.5	9.5	324.0	2.0	0.8	0.2	28.7
17	2911.8	440.0	8.7	104.8	5.1	44.5	9.5	324.0	2.0	1.0	0.2	28.7
18	3494.1	440.0	8.7	104.8	5.1	44.5	9.5	324.0	2.0	1.2	0.2	28.7
19	579.5	491.9	7.8	104.8	5.1	44.5	9.5	324.0	2.5	0.2	0.2	32.1
20	1159.1	491.9	7.8	104.8	5.1	44.5	9.5	324.0	2.5	0.4	0.2	32.1
21	1738.6	491.9	7.8	104.8	5.1	44.5	9.5	324.0	2.5	0.6	0.2	32.1
22	2318.1	491.9	7.8	104.8	5.1	44.5	9.5	324.0	2.5	0.8	0.2	32.1
23	2897.6	491.9	7.8	104.8	5.1	44.5	9.5	324.0	2.5	1.0	0.2	32.1
24	3477.2	491.9	7.8	104.8	5.1	44.5	9.5	324.0	2.5	1.2	0.2	32.1
25	594.1	538.8	7.1	104.8	5.1	44.5	9.5	324.0	3.0	0.2	0.2	35.1
26	1188.3	538.8	7.1	104.8	5.1	44.5	9.5	324.0	3.0	0.4	0.2	35.1
27	1782.4	538.8	7.1	104.8	5.1	44.5	9.5	324.0	3.0	0.6	0.2	35.1
28	2376.6	538.8	7.1	104.8	5.1	44.5	9.5	324.0	3.0	0.8	0.2	35.1
29	2970.7	538.8	7.1	104.8	5.1	44.5	9.5	324.0	3.0	1.0	0.2	35.1
30	3564.9	538.8	7.1	104.8	5.1	44.5	9.5	324.0	3.0	1.2	0.2	35.1

(Continued)

No.	a [mm]	b_p [mm]	t_p [mm]	h_w [mm]	t_w [mm]	b_f [mm]	t_f [mm]	σ_{Yeq} [MPa]	β	λ	A_s/A	b_t [mm]
31	575.9	582.0	6.6	104.8	5.1	44.5	9.5	324.0	3.5	0.2	0.2	38.0
32	1151.7	582.0	6.6	104.8	5.1	44.5	9.5	324.0	3.5	0.4	0.2	38.0
33	1727.6	582.0	6.6	104.8	5.1	44.5	9.5	324.0	3.5	0.6	0.2	38.0
34	2303.4	582.0	6.6	104.8	5.1	44.5	9.5	324.0	3.5	0.8	0.2	38.0
35	2879.3	582.0	6.6	104.8	5.1	44.5	9.5	324.0	3.5	1.0	0.2	38.0
36	3455.2	582.0	6.6	104.8	5.1	44.5	9.5	324.0	3.5	1.2	0.2	38.0
37	574.6	622.2	6.2	104.8	5.1	44.5	9.5	324.0	4.0	0.2	0.2	40.6
38	1149.2	622.2	6.2	104.8	5.1	44.5	9.5	324.0	4.0	0.4	0.2	40.6
39	1723.7	622.2	6.2	104.8	5.1	44.5	9.5	324.0	4.0	0.6	0.2	40.6
40	2298.3	622.2	6.2	104.8	5.1	44.5	9.5	324.0	4.0	0.8	0.2	40.6
41	2872.9	622.2	6.2	104.8	5.1	44.5	9.5	324.0	4.0	1.0	0.2	40.6
42	3447.5	622.2	6.2	104.8	5.1	44.5	9.5	324.0	4.0	1.2	0.2	40.6